THE ASTROPHYSICAL JOURNAL, 281: 158–171, 1984 June 1

COLOR-MAGNITUDE PHOTOMETRY FOR THE GLOBULAR CLUSTER NGC 288

EDWARD W. OLSZEWSKI
Department of Astronomy, University of Washington, and Dominion Astrophysical Observatory, Herzberg Institute of Astrophysics

R. CANTERNA[1]
Department of Physics & Astronomy, University of Wyoming

AND

WILLIAM E. HARRIS
Department of Physics, McMaster University

Received 1982 May 10; accepted 1983 November 29

ABSTRACT

We describe new photographic *BV* color-magnitude photometry for the globular cluster NGC 288, covering the magnitude range $13 < V < 21$ (from the red-giant tip to about 2 mag below the main-sequence turnoff).

We find the turnoff (bluest point on the observed main sequence) to lie at $V \approx 19.1$, $(B-V) \approx 0.44$, about 0.3 mag fainter than previously estimated by Alcaino and Liller but in close agreement with two other more recent studies. Within the internal scatter of measurement, our C-M diagram can be successfully matched by VandenBerg isochrones with relatively "normal" abundance and age parameters ($Z \approx 0.001$, $Y \approx 0.2$, age $\approx 15 \times 10^9$ yr).

Subject headings: clusters: globular — photometry — stars: evolution

I. INTRODUCTION

The halo cluster NGC 288 (C050−268) has recently and rapidly become an object of some importance in our attempts to understand the chemical compositions of globular clusters. Since the discovery that at least one other parameter besides Z (i.e., [Fe/H]) was needed to reproduce the observed color-magnitude diagrams (CMDs) of all globular clusters (see, e.g., Faulkner 1966; Sandage and Wildey 1967), several possibilities for second and third parameters have been advanced, primarily including age, CNO abundance, and helium abundance. $Z_{\rm CNO}$ has become perhaps the leading candidate (e.g., see, Pilachowski, Wallerstein, and Leep 1980; Cohen 1980; Demarque 1980; Pilachowski, Sneden, and Wallerstein 1983 [hereafter PSW]; see also Suntzeff 1981; McClure and Hesser 1981; Cohen and Frogel 1982, and Friel *et al.* 1982, for more discussions of CNO and the second parameter problem). This is because age alone cannot account entirely for the variety of CMD "anomalies" (giant-branch and turnoff colors, distribution of stars along the horizontal branch [HB]) that have been observed to date (cf. Carney 1980), and the helium composition can be investigated only indirectly and with great difficulty (Deupree *et al.* 1978; Green 1980; Demarque and McClure 1980). The suggested revisions in the fundamental spectroscopic abundance determinations for globular clusters giants (e.g., Cohen 1978, 1979, 1980; Pilachowski, Sneden, and Canterna 1980; Pilachowski, Wallerstein, and Leep 1980; Bell and Gustaffson 1982; PSW) which indicate that [O/Fe] ranges from ~0.0 to 0.5 in globular clusters have added to the suspicion that $Z_{\rm CNO}$ may be the most important second parameter, and in some sense may even be more important than the "first" parameter Z, in terms of controlling the distribution of HB stars especially. At the same time, recent discussions of globular cluster ages and isochrone fits to globular cluster main sequences now suggest (Sandage 1982; VandenBerg 1983) that all clusters studied to date can be successfully, if approximately, fitted by a single age near 15 billion years.

The possibility has been raised that NGC 288 may stand in opposition to the $Z_{\rm CNO}$ second-parameter trend. The first color-magnitude studies of NGC 288, by Cannon (1974) and Menzies (1972, unpublished), showed that its CMD is basically of the M13 type, which is characterized by a heavily populated blue horizontal branch with virtually no RR Lyrae members or red HB stars. However, as Cannon discussed, NGC 288 essentially represents one extreme of this class since its giant-branch color $(B-V)_{o,g}$ (Sandage and Smith 1966) is redder than that of M13 or any other globular clusters of this same HB type. In addition, abundance measurements from high-dispersion spectra of giants in NGC 288 (Pilachowski and Sneden 1980; PSW) yield $[{\rm Fe/H}] = -1.2$, $[{\rm O/H}] = -0.7$. These values closely resemble those for 47 Tuc as derived by the same technique (Pilachowski, Sneden, and Canterna 1980; PSW). Thus the presence of a strong blue HB is difficult, if not impossible, to understand if these relatively high [Fe/H] abundances are correct.

An additional type of observation which might be expected to help disentangle the effects of Z, $Z_{\rm CNO}$, helium, and age would be photometry covering the main-sequence and turnoff regions of the CMD. Alcaino and Liller (1980*b*) and Cannon (1981) have obtained data of this type and directed their discussions primarily to a determination of the cluster age. In this paper we wish to present the results of an independent color-magnitude study of NGC 288 and to concentrate on its implications for the cluster composition as well as the age. Our new main-sequence photometry in particular strengthens the idea that NGC 288 may be an important object within the general metallicity sequence occupied by the globular clusters.

II. COLOR-MAGNITUDE DATA

To calibrate our own color-magnitude measurements in the *BV* system we relied first on the photoelectric sequence of

[1] Visiting Astronomer, Cerro Tololo Inter-American Observatory, which is operated by the Association of Universities for Research in Astronomy, Inc., under contract with the National Science Foundation.

1984ApJ...281..158O

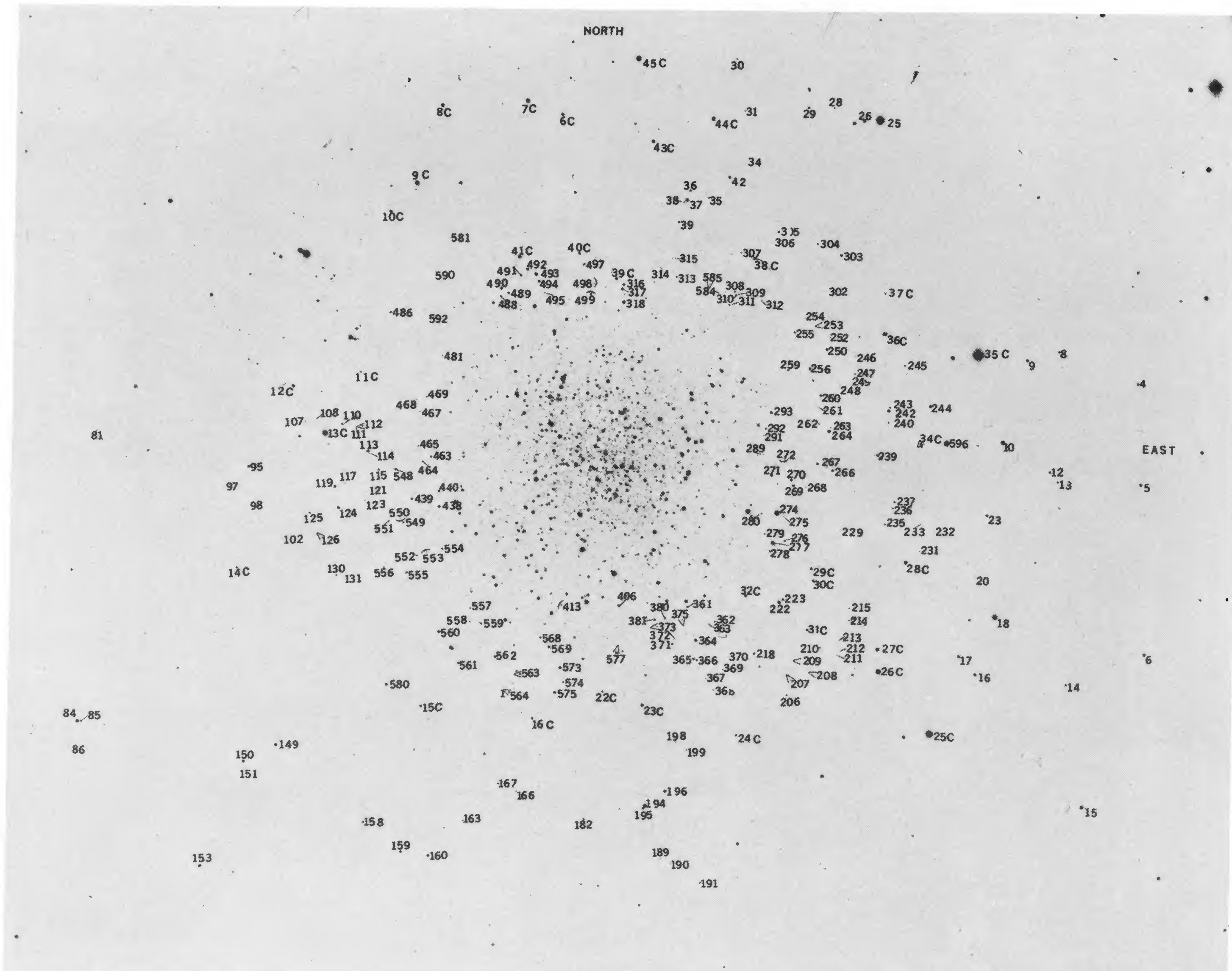

FIG. 1.—Identification chart for the Cannon photoelectric standards (indicated by a C following the number) and the photographically measured stars with $V < 17.0$ (Table 3D) of NGC 288.

47 stars in the NGC 288 field published by Cannon (1974). However, to make an extra check on this sequence and also to add a few more blue HB stars to the calibration, we carried out some additional *BV* photoelectric observations at CTIO in 1976 August (0.6 m telescope) and 1977 September (1.5 m telescope). These measurements are summarized in Table 1 and compared with Cannon's results for the stars in common. In the table, the star numbers follow Cannon, except for the last four which are identified in Figure 1. We regard the agreement between our data and Cannon's as satisfactory, considering the different equipment and the crowding problems for some stars; within the internal errors there are no significant zero-point shifts or trends with magnitude.

All the photographic plates for our C-M study were obtained at CTIO, with the 1 m and 4 m telescopes and one additional plate from the 1.5 m. This material is summarized in Table 2 and falls into two principal groups: the 4 m plates were used almost solely for the main-sequence photometry ($V > 17$), whereas the 1 m plates were used to define the brighter sections of the CMD. Three short-exposures *B* plates (numbers Y1649, Y1667, and Y1697) were kindly loaned to us by Dr. Martha Liller.

Most of the plates (including all 4 m exposures) were taken with the auxiliary 16 cm Pickering-Racine prism which produces secondary images of the brighter stars in the field to help extend the photometric calibrations to the plate limits (Pickering 1891; Racine 1969; Blanco 1982; Christian and Racine 1983). The magnitude difference Δm between primary and secondary images for the 4 m plates was calibrated from the well-studied 47 Tuc field (Lee 1977; Hesser and Hartwick 1977), photographed during the same nights as NGC 288. The extensive photoelectric photometry in the 47 Tuc field yielded a value of $\Delta m = 6.82$. The Δm value for the 1.0 m plates was small enough to be calibrated directly on the NGC 288 field since a large overlap with the photoelectric sequence existed. We found an average value of $\Delta m = 3.66$ for the 1.0 m plates.

TABLE 1

PHOTOELECTRIC BV PHOTOMETRY

Star	V	$B-V$	n	ΔV^a	$\Delta(B-V)^a$
3	13.17	0.95	1	0.04	0.02
6	15.18	0.89	2	−0.02	0.17
7	13.95	1.32	1	0.01	0.00
10	15.21	1.48	2	−0.01	0.01
14	16.41	−0.07	2	0.07	−0.02
20	13.03	1.37	2	0.00	0.01
23	14.98	0.89	2	0.06	−0.05
25	11.70	0.60	2	0.02	−0.03
27	14.28	0.68	1	−0.01	0.01
28	14.70	0.93	1	0.07	−0.08
31	15.91	−0.05	1	−0.02	−0.01
36	13.88	1.14	1	0.01	−0.01
39	15.63	0.85	1	0.03	0.04
42	15.93	0.03	2	−0.07	0.12
44	14.03	1.46	1	0.03	0.02
45	12.83	0.88	1	−0.01	0.04
421	15.34	0.16	2		
457	15.36	0.18	2		
492	15.77	0.00	2		
504	16.15	−0.09	2		

[a] Differences are in the sense (OCH − Cannon).

TABLE 2

PHOTOGRAPHIC PLATE DATA

Plate	Telescope	Exp	Color	Wedge
4356	4 m	15 min	*V*	yes
4357	4 m	20 min	*V*	yes
4358	4 m	20 min	*B*	yes
4359	4 m	15 min	*B*	yes
C-111	1.5 m	15 min	*V*	no
398	1 m	60 min	*V*	yes
400	1 m	60 min	*B*	yes
1109	1 m	75 min	*V*	yes
Y-1649	1 m	10 min	*B*	no
Y-1667	1 m	10 min	*B*	no
Y-1697	1 m	10 min	*B*	no

All of the plates were measured with the Cuffey-type iris photometer at the University of Washington. The brighter ($V < 18.2$) parts of the CMD were defined by selection of a homogeneous sample of stars from $\approx 75''$ out to 7′.5 from the cluster center, whereas the deeper main-sequence photometry came from a sample of stars on the north side of the cluster between radii 7′.2 and 8′.8. Identification charts for the photographically measured stars are given in Figures 1 to 4, and the final reduced *BV* data in Table 3. For the iris photometry reductions we used the CMDGRM program (Stetson and Harris 1977; Harris and Pateman 1979), executed separately for the 4 m plates (main-sequence stars) and the others (bright stars) since the two plate measurement series had few stars in common. To ensure particularly that no programming errors would affect the critical main-sequence data, the 4 m plates were reduced independently at Washington and at McMaster through different operating versions of the same program. The results proved to be identical to within the internal errors of the data (± 0.02 mag) and the data summarized in Table 3 are the averages of the two reductions.

We were able to make an additional and valuable check on the faint calibration by adding in a video-camera *V*-magnitude sequence of stars obtained in the NGC 288 field by Butcher (1980). From his sequence we used 10 stars in the range $18.5 < V < 20.5$, which brackets the important turnoff region of the CMD. Since the Butcher standards contain only *V* magnitudes and not *B*, we made a preliminary reduction including them as "program" stars to estimate their $B-V$ colors, and then reinserted them as standards with their photographically estimated $B-V$ values for the final reduction. Our results for these extra standards are summarized in Table 4. In general, the magnitude scale of the secondary images agreed systematically with the Butcher standards: for the 10 Butcher stars we used, we found $\Delta V(\text{pg}-\text{Butcher}) = -0.040 \pm 0.225$, or 0.017 ± 0.10 if the three most deviant stars are excluded (cf. Table 4). We therefore believe our main-sequence magnitude scale to be systematically correct to within ± 0.20 mag.

Table 3A contains the "photographically smoothed" measurements of our standard stars: numbers 3–45 are from Cannon (1974); the four stars with numbers 421–504 are our extra standards from Table 1. In Tables 3B and 3C, the faint sample of photographically measured stars (mostly $V > 18$, from Figs. 3 and 4) for the two separate quadrants is listed. Finally, Table 3C contains the data for the bright sample of stars (Fig. 2).

The random internal errors of the data in Table 3 are near

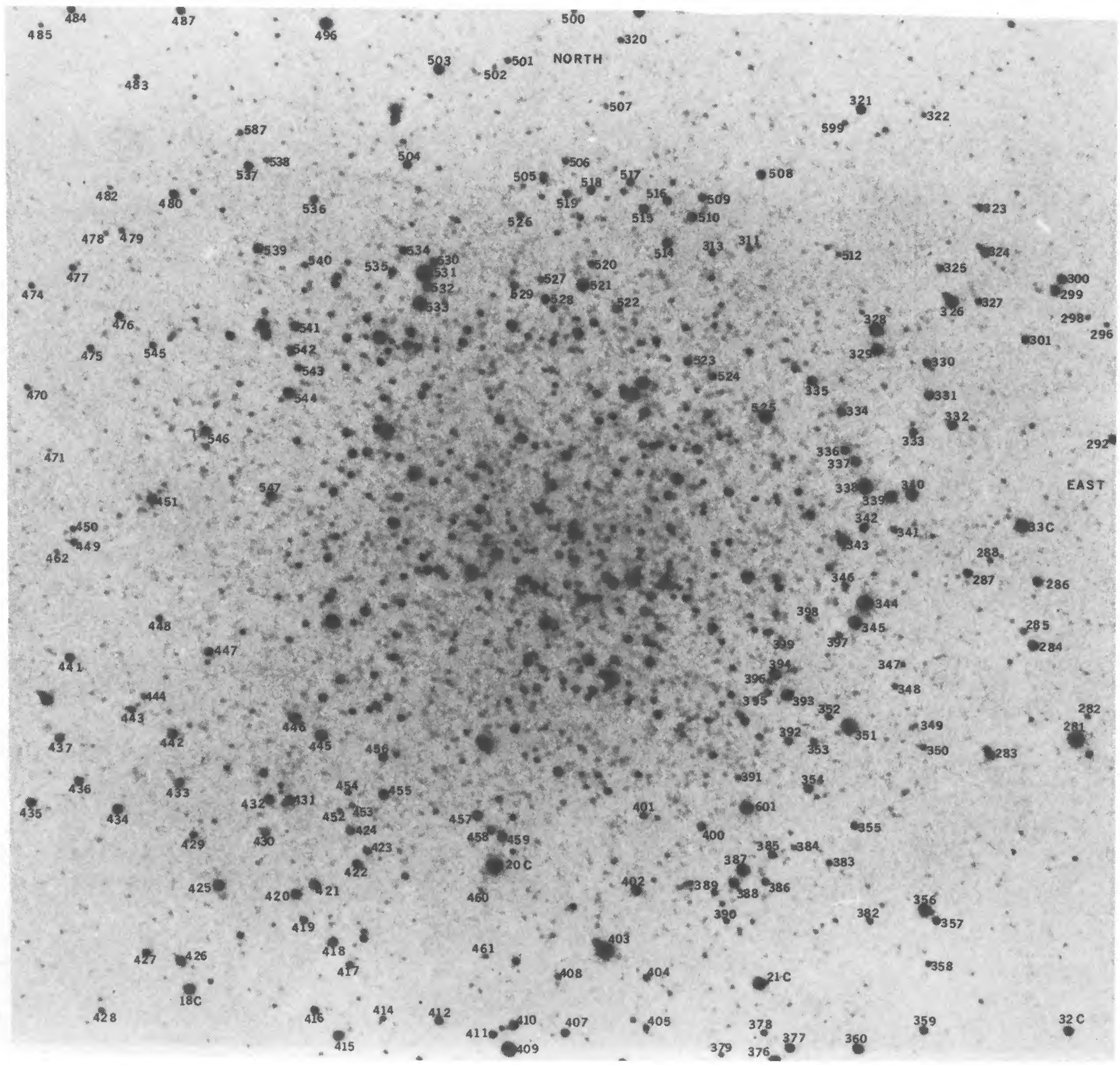

FIG. 2.—Identification chart for the inner region of NGC 288 for the Cannon standards (Table 3A) and the photographically measured stars in Table 3D.

1984ApJ...281..158O

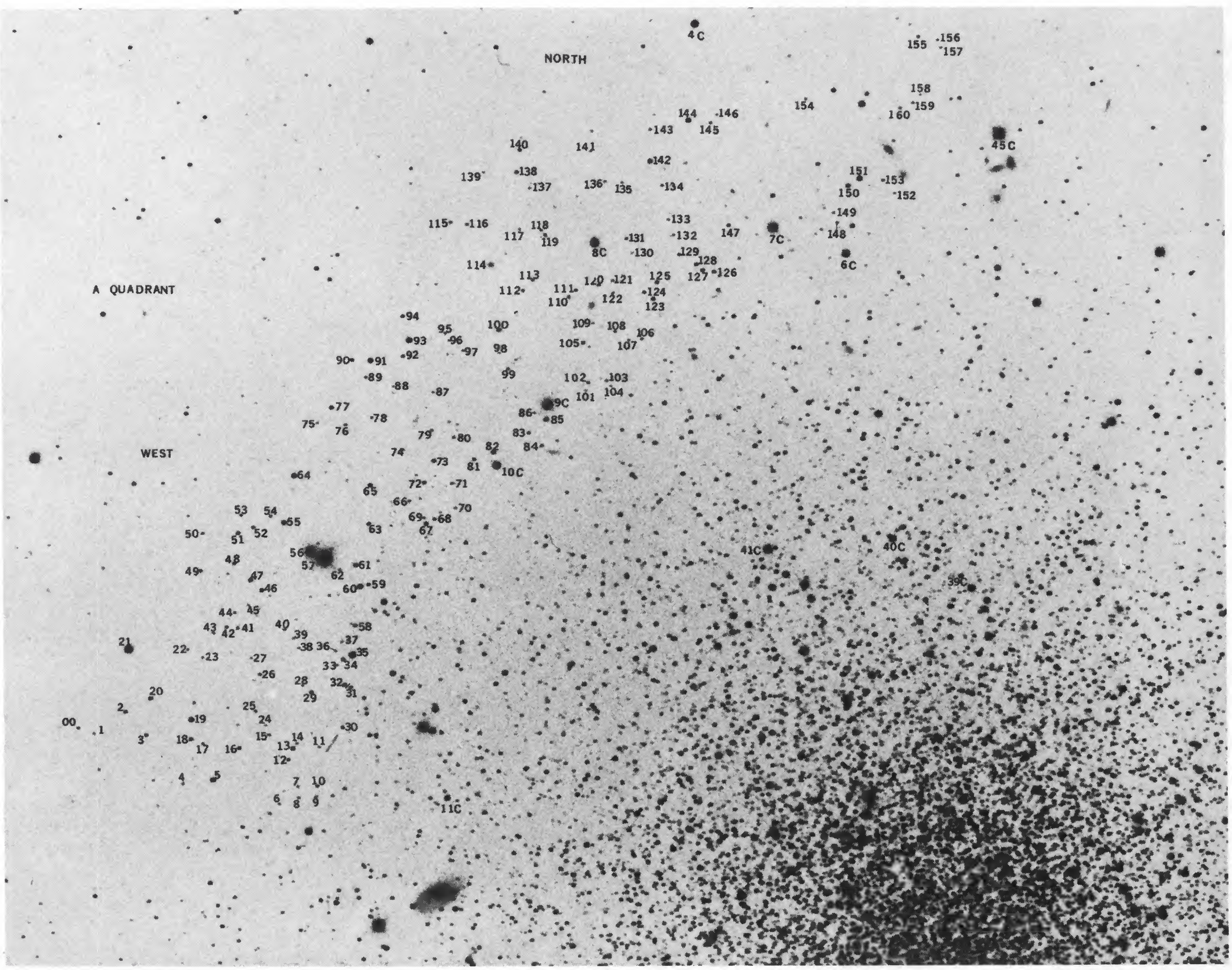

FIG. 3.—Identification chart for stars in Quadrant A (Table 3B)

1984ApJ...281..158O

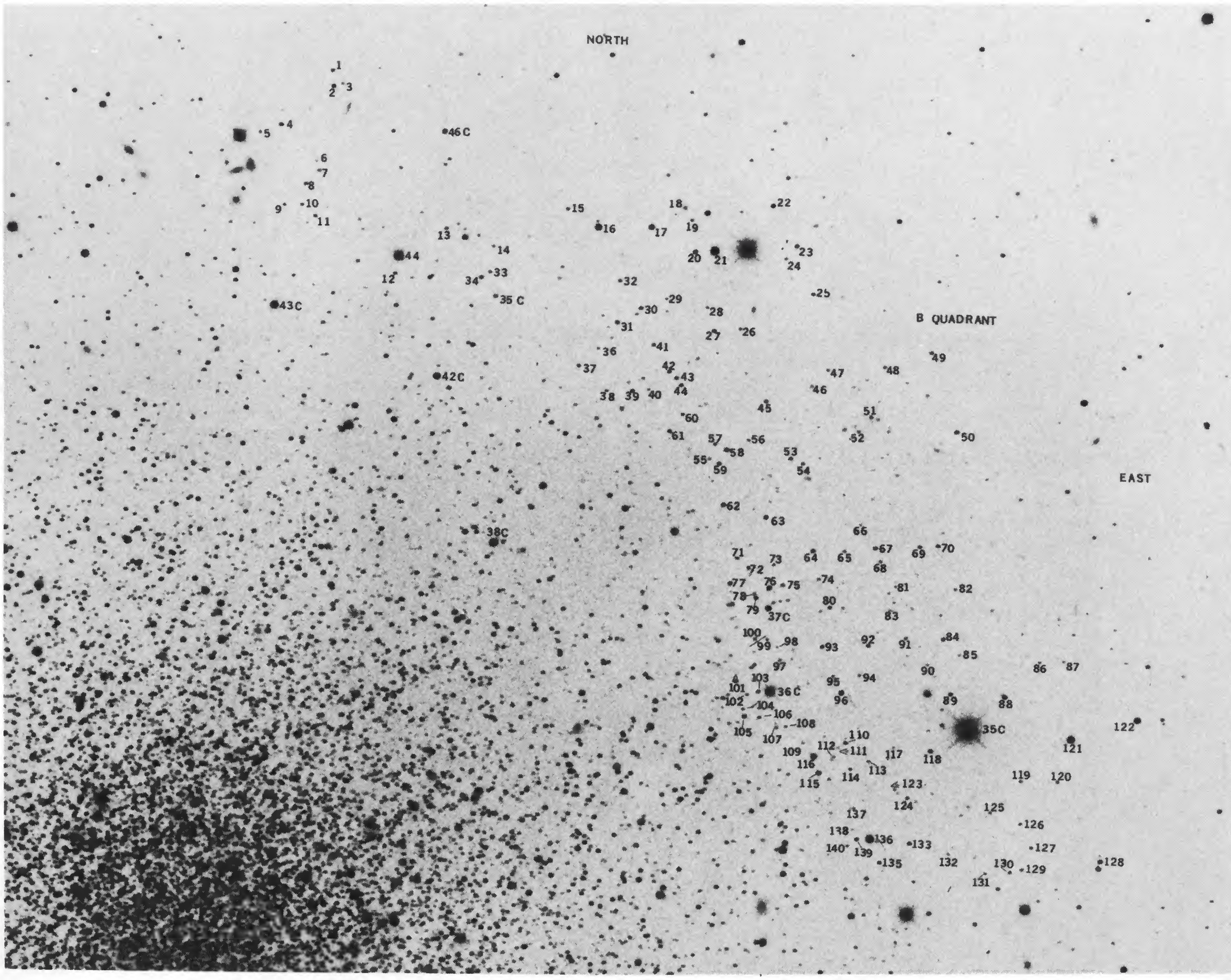

FIG. 4.—Identification chart for stars in Quadrant B (Table 3C)

TABLE 3A

PHOTOGRAPHIC PHOTOMETRY OF STANDARD STARS

STAR	V	B-V	STAR	V	B-V	STAR	V	B-V
3C	13.17	1.03	4C	15.30	.55	5C	16.21	.92
6C	15.17	.93	7C	13.90	1.31	8C	14.25	.82
9C	13.47	.69	10C	15.22	1.39	11C	17.21	.74
12C	15.56	.80	13C	12.58	.45	14C	16.60	-.09
15C	16.70	-0.08	16C	16.98	-.13	17C	14.69	.61
18C	14.85	.90	19C	14.60	.88	20C	12.96	1.39
21C	14.08	.52	22C	16.98	.75	23C	14.97	.85
24C	16.60	.75	25C	11.70	.60	26C	12.78	.69
27C	14.38	.60	28C	14.76	.91	29C	15.44	1.13
30C	15.84	.87	31C	15.98	.03	32C	15.39	.93
33C	14.01	.94	35C	10.28	.56	36C	13.86	1.13
37C	17.15	-.11	38C	14.98	.83	39C	15.53	.85
40C	15.65	.08	41C	14.44	.92	42C	15.94	.02
43C	14.92	1.42	44C	13.98	1.50	45C	12.81	.85
46C	17.45	.76	457	15.03	.35	492	15.83	.04
504	16.01	-.01	421	15.20	.08			

TABLE 3B

PHOTOGRAPHIC PHOTOMETRY OF STARS IN QUADRANT A

STAR	V	B-V	STAR	V	B-V	STAR	V	B-V
00	20.19	.70	01	20.93	.79	02	19.66	.56
04	20.61	.74	05	17.70	.67	06	20.98	.80
07	20.95	.96	08	20.40	.64	09	20.26	.37
10	20.44	.41	11	20.90	.79	12	19.89	.45
13	18.38	.60	14	20.80	.89	15	20.50	.57
16	19.45	.35	17	20.85	.77	18	19.24	.46
19	17.25	.87	20	18.86	.42	21	15.05	.66
22	20.86	.59	23	20.89	1.16	24	21.09	.80
25	20.54	.68	26	20.32	.50	27	21.08	.87
28	20.94	.45	29	19.12	.48	30	19.68	.39
31	19.83	.52	32	18.74	.43	33	20.75	.82
34	18.97	.40	35	16.07	.71	36	20.97	.65
37	20.66	.57	38	20.96	.68	39	21.12	.80
40	20.52	.46	41	19.81	.56	42	19.78	.45
43	20.62	.67	44	20.43	.60	45	21.19	.83
46	18.88	.48	47	19.04	.32	48	20.11	.40
49	19.75	.67	50	20.46	.71	51	18.93	.41
52	19.83	.37	53	20.44	.63	56	13.23	.43
57	11.43	.97	58	19.18	1.44	59	19.61	.44
60	17.22	.61	61	18.39	.42	62	20.71	.54
63	19.40	.45	64	17.31	-.17	65	18.73	.49
66	20.65	.86	67	18.62	.53	68	19.86	.41
69	20.60	.60	70	20.80	.71	71	20.23	.71
72	19.54	.46	73	18.78	.39	74	20.79	.81
75	20.95	.78	76	20.47	.75	77	19.03	.38
78	20.70	.72	79	20.28	.61	80	20.13	.43
81	19.55	.42	82	18.39	.60	83	19.98	.71
84	20.07	.47	85	17.85	.67	86	20.85	.73
87	20.76	.65	88	21.01	1.08	89	20.19	.51
90	19.42	.50	91	17.55	1.55	92	19.82	.45
93	16.65	.60	94	19.28	.65	95	20.38	.64
96	20.95	.85	97	20.66	.58	98	21.01	.90
99	20.96	1.04	101	21.07	.87	102	20.11	.61
103	20.57	1.46	104	21.02	.80	105	19.49	.35
106	20.45	.61	107	20.82	.82	108	20.46	.60
109	21.05	.60	110	20.23	1.63	111	19.85	.67
112	20.08	.62	113	20.44	.51	114	19.66	1.83
115	20.30	.56	116	20.13	1.50	117	20.74	.96
118	20.46	.75	119	19.93	1.61	120	20.10	.49
121	20.43	.69	122	20.58	.62	123	18.70	.51
124	19.59	.50	125	19.16	.49	126	19.34	.41
127	18.83	.54	128	18.95	.68	129	20.00	.55
130	21.15	.84	131	20.05	.57	132	20.80	.73
133	20.68	.77	134	20.37	.70	135	20.77	.69
136	20.77	.83	137	20.72	1.28	138	19.14	.29
139	20.96	.73	140	19.53	.48	141	21.03	.84
142	18.02	.68	143	20.33	.61	144	17.52	.81
145	20.23	.57	146	20.85	.66	147	19.44	.47
148	20.60	.55	149	20.65	.69	150	18.44	.62
151	17.09	.72	152	20.80	.77	153	19.96	.78
154	20.41	.49	155	19.79	.53	156	20.67	.45
157	20.78	.84	158	21.17	.94	159	20.33	.45
160	20.35	.40	174	21.03	.75	175	20.46	.62
176	19.96	.43						

TABLE 3C

PHOTOGRAPHIC PHOTOMETRY OF STARS IN QUANDRANT B

STAR	V	B-V	STAR	V	B-V	STAR	V	B-V
01	19.43	.46	02	18.70	.51	03	20.64	.67
04	18.75	1.46	05	20.17	.62	06	21.06	1.02
07	20.35	1.38	08	19.31	.55	09	20.29	.44
10	20.13	.60	11	19.73	.60	12	19.68	.51
13	19.96	.50	14	20.57	.58	15	19.93	.57
16	15.99	.76	17	17.28	.79	18	20.36	1.41
19	20.27	.61	20	18.36	.61	21	14.69	.94
22	18.43	.45	23	18.77	.49	24	20.84	.78
25	19.69	.61	26	20.43	.41	27	18.83	.50
28	20.64	.70	29	20.91	.73	30	19.15	.55
31	18.99	.48	32	19.53	.54	33	20.12	.67
34	19.16	.52	35	19.35	1.51	36	20.73	.65
37	19.61	.51	38	20.51	.53	39	18.83	.57
40	20.76	.75	41	19.64	.42	42	19.53	.38
43	19.31	.59	44	19.34	.50	45	19.16	.50
46	20.78	1.49	47	20.64	1.65	48	19.92	.54
49	19.48	.35	50	18.70	.38	51	20.30	1.86
52	20.53	.88	53	19.57	.31	54	19.99	.36
55	20.80	.57	56	20.68	.74	57	20.27	.53
58	18.20	.68	59	18.90	.47	60	20.10	1.67
61	19.57	.33	62	18.19	.62	63	18.73	.57
56	20.68	.74	57	20.27	.53	58	18.20	.68
59	18.90	.47	61	19.57	.33	62	18.19	.62
63	18.73	.55	64	18.73	.43	65	20.42	.54
66	21.02	1.29	67	18.97	.39	68	20.46	1.65
69	19.53	.50	70	19.54	.35	71	20.00	.48
72	19.70	.49	73	20.68	.68	74	20.37	.56
75	19.73	.47	76	18.10	.41	77	18.71	.52
78	20.31	.82	79	19.37	.39	80	19.93	.33
81	20.86	1.41	82	20.67	.51	84	19.06	.47
85	20.99	.89	86	20.57	.53	87	20.93	.68
88	18.28	.47	89	19.15	.36	90	20.81	.79
91	20.48	.60	92	19.67	.45	93	19.62	.35
94	20.51	.49	95	20.80	.75	96	17.63	1.18
97	20.60	.49	98	21.38	.83	99	20.53	.44
100	20.04	.46	101	19.07	.49	102	20.76	.74
103	19.28	.37	104	20.67	.66	105	18.94	.40
106	20.40	.49	107	20.30	.65	108	20.59	.55
109	21.06	1.17	110	19.58	.35	111	20.97	.71
112	20.85	.63	113	20.87	.47	114	20.20	.50
115	17.99	.78	116	17.07	-.13	117	21.09	.87
118	18.54	.39	119	20.34	.38	120	20.46	1.04
121	15.51	1.16	122	16.32	.77	123	20.84	.54
124	19.88	.43	125	20.83	.82	126	20.50	.61
127	20.27	.60	128	18.19	.56	129	20.22	.55
130	20.04	.72	132	20.85	.83	133	18.94	.52
135	19.26	.40	136	15.10	.87	137	20.77	.52
138	21.28	.92	139	19.01	.60	140	20.86	.75
141	11.15	.55						

$\sigma(V) = \pm 0.03$, $\sigma(B-V) = \pm 0.04$ (though somewhat smaller than this for $V < 15$, and larger for $V > 17$ [bright sample] and $V > 20$ [faint sample] because of the coverage of the plate material).

An additional electronographic sequence in the region has been published by Hawkins (1979, 1981; his SGP1 sequence) and was used by Alcaino and Liller (1980*b*) in their color-magnitude study. We also measured this sequence as part of the total reduction but did not use it in the final calibration because the scatter for these sequence stars appeared to be somewhat larger than for the Butcher sequence and the secondary images.

The photographic "color equations" or transformations from the natural magnitude system of the emulsion/filter combinations used are a final necessary ingredient for the photographic reduction. If these are expressed as $m_{pg} = m + k(B-V)$, for the 4 m plates we determined the coefficients k to be $k_V = -0.03 \pm 0.02$, $k_B = 0.01 \pm 0.02$, and for the 1 m plates $k_V = -0.08 \pm 0.04$, $k_B = 0.00 \pm 0.02$. These agree well with other determinations in the literature for the same telescopes (e.g., Alcaino and Liller 1980*a*; Harris and Canterna 1980; Stetson and Harris 1977), and we believe no noticeable errors have entered due to this source alone. In particular, the colors of the main-sequence stars are virtually independent of the adopted k's since they are near the average color of all the stars in the CMD.

III. THE COLOR-MAGNITUDE DIAGRAM AND REDDENING

Our results for the total CMD are shown in Figure 5. Since the 1 m plates cut off at $V > 17$, the data have a larger scatter there and the subgiant branch just below it is poorly defined. However, the 1 m data do sample almost the entire cluster and consequently the horizontal branch (HB) and upper gaint branch are well defined. From Cannon's (1974) photoelectric survey alone, it was not clear where the brightest part of the blue HB actually leveled off (if at all) because of the small number of stars. From our larger photographic sample, we see that the HB does indeed reach a nearly level stage near the RR Lyrae blue edge, at $V_{HB} = 15.3 \pm 0.1$. The sections of the HB containing the RR Lyrae region and redward are, however, vacant; only one RR Lyrae is known in the entire cluster (Hollingsworth and Liller 1978). The one known long-period variable (Sawyer Hogg 1973) appears to define the red tip of the giant branch in our diagram.

Mean lines for the total CMD are listed in Table 5. The brighter sections (GB and HB) agree well (necessarily) with Cannon's sequences, whereas the fainter ($V > 17.5$) sections depend entirely on the calibrations discussed in the previous

TABLE 3D

PHOTOGRAPHIC PHOTOMETRY OF STARS BRIGHTER THAN $V = 18.2$

STAR	V	B-V	STAR	V	B-V	STAR	V	B-V
004	16.27	1.34	005	15.85	1.45	006	15.63	.74
008	16.41	.80	009	15.61	1.31	010	13.87	1.07
012	16.74	.80	013	17.14	.86	014	16.46	.33
015	14.56	.52	016	15.25	.37	017	15.31	.94
018	12.73	.51	020	18.00	.97	023	15.70	-.02
025	11.16	.54	026	14.68	.96	028	17.48	.76
029	16.10	.79	030	17.63	.78	031	17.41	.81
034	18.20	.63	035	17.18	.79	036	16.76	.94
037	14.53	.81	038	17.41	.66	039	16.54	-.13
084	14.67	.74	085	17.02	.92	086	17.84	.77
095	15.64	.84	097	18.21	.78	098	18.15	.75
102	18.20	.75	107	17.65	.79	108	17.85	1.55
110	16.72	.58	111	18.15	.65	112	17.34	.74
113	15.87	.88	114	18.12	.68	115	16.73	-.13
117	17.87	.72	119	15.83	.78	121	18.18	.71
123	17.91	.82	124	15.73	1.25	125	17.05	.84
126	18.15	.75	130	17.45	.81	131	18.19	.80
149	15.16	.88	150	15.73	1.34	151	18.13	.66
153	15.36	1.08	158	16.95	.75	159	16.00	-.08
160	15.89	-.03	163	17.44	-.09	166	17.72	.69
167	17.05	.81	182	16.97	-.25	189	17.59	1.15
190	17.11	1.55	191	17.11	1.26	194	13.95	1.09
195	16.15	1.08	196	15.37	.74	198	17.89	.69
199	17.91	.34	206	17.44	.74	207	17.77	.89
208	18.23	.82	209	18.23	.78	210	17.49	.76
211	17.99	.72	212	18.23	.73	213	18.19	.71
215	17.74	.68	218	16.55	-.13	222	14.86	.96
223	15.84	-.05	229	18.10	.75	231	17.89	.59
232	18.21	.59	233	18.24	.78	234	18.24	.81
235	17.30	.83	236	17.40	.73	237	17.00	.75
239	15.63	.89	240	17.43	.71	242	17.12	-.10
243	17.48	.78	244	15.07	.92	245	17.11	-.19
246	18.15	.74	247	17.53	.67	248	18.04	.65
249	18.20	.70	250	15.94	-.07	252	18.06	.74
253	18.20	.75	254	18.22	.79	255	16.91	-.15
256	15.91	-.07	259	16.95	.74	260	16.23	.85
261	18.18	.81	262	17.68	.70	263	17.59	.73
264	15.13	.88	265	18.18	.56	266	16.18	.80
267	16.42	.80	268	17.90	.75	269	15.75	.01
270	16.16	.83	271	15.57	.85	272	17.89	.74
274	13.05	1.41	275	18.06	.71	276	16.66	.82
277	14.03	1.02	278	16.63	.80	279	17.02	-.06
280	17.51	.74	281	13.27	1.28	282	17.51	.24
283	15.53	.86	284	15.04	.54	285	17.02	.70
286	15.62	.85	287	15.79	-.03	288	17.36	.73
289	18.04	.60	290	18.03	.77	291	17.05	.77
292	15.83	.84	293	16.11	.89	296	17.72	.63
297	17.77	.75	298	17.70	.64	299	15.48	.81
300	15.39	.90	301	15.84	-.04	302	18.16	.67
303	16.71	.87	304	17.33	1.18	305	16.38	.75
306	18.15	.71	307	17.61	.71	308	17.34	.86
309	17.66	.65	310	16.60	-.08	311	16.90	.80
312	17.77	.70	313	17.28	.76	314	17.84	.74
316	16.11	-.09	317	16.06	-.09	318	15.17	.89
320	17.09	.78	321	15.46	.84	322	17.62	.74
323	16.33	-.13	324	15.41	.88	325	16.45	-.11
326	14.32	.70	327	16.47	-.18	328	14.19	1.07
329	14.52	.84	330	16.03	.85	331	15.48	.84
332	15.57	.92	333	16.03	.04	335	15.47	.87
336	15.93	.88	337	15.49	.06	338	13.63	1.17
339	14.47	.79	340	14.37	1.02	341	16.96	.68
342	15.82	-.01	343	14.52	1.01	344	13.27	1.27
345	14.09	1.04	346	16.51	-.10	347	17.55	.69
348	17.19	.78	350	17.20	.71	351	13.54	1.18
352	16.83	.67	353	16.79	.73	354	15.75	-.04
355	16.24	.86	357	15.96	-.03	358	17.08	.82

section. We find the main-sequence turnoff point (defined as the bluest point reached on the main sequence) to be at $V_{\rm to} = 19.1 \pm 0.1$, $(B-V)_{\rm to} = 0.44 \pm 0.03$. This position is fainter by 0.3 mag than was estimated by Alcaino and Liller (1980*b*), as well as slightly bluer, by -0.06 mag in $B-V$. The reason for this difference appears to be mainly that our data contain somewhat lower scatter and reach ~ 1 mag fainter than theirs, so that the entire turnoff region is more clearly defined here. Random errors aside, there do not appear to be major systematic differences between these two faint sets of photometry: for 58 stars fainter than $V \approx 17$ in common with Alcaino and Liller we find mean differences of $\Delta V(\text{0CH}-\text{AL}) = +0.059 \pm 0.019$, $\Delta(B-V)(\text{0CH}-\text{AL}) = 0.036 \pm 0.014$. This agreement is encouraging, but not entirely surprising since certain calibration techniques and standard stars were used in both studies.

Rougher comparisons with other recent photometric studies of the NGC 288 main sequence can also be made here. Cannon (1981) discusses a preliminary analysis of photographic and electronographic photometry which places the turnoff at $V_{\rm to} \approx 19.2$, $(B-V)_{\rm to} \approx 0.6$, at about the same magnitude level as ours but ~ 0.2 mag redder.[2] Harris, Hesser, and Atwood (1983), from SIT vidicon photometry of a sample

[2] Cannon and Hawkins (1983) note that this apparent systematic difference has now been resolved by a recalibration and measurement of a much larger sample of stars with their electronographic technique.

TABLE 3D—*Continued*

STAR	V	B-V	STAR	V	B-V	STAR	V	B-V
359	16.02	.85	360	14.95	.91	361	17.00	.69
362	17.16	.74	363	17.43	.75	364	14.37	.10
365	15.98	-.10	366	17.10	.60	367	17.82	.72
368	17.58	.70	369	17.81	.69	370	18.13	.62
371	15.89	.58	372	17.43	.75	373	17.49	-.14
375	18.04	.67	376	15.28	.01	377	15.34	.10
378	16.82	.71	379	17.27	.85	380	16.04	.88
381	17.08	-.13	382	16.92	.67	383	18.16	.59
384	16.93	.79	385	15.92	-.09	386	16.51	.84
387	14.26	1.00	388	15.42	.89	389	16.83	.83
390	17.13	.72	391	16.99	-.13	392	16.07	-.05
393	14.83	1.00	394	14.62	.95	395	16.68	.73
396	16.99	-.28	397	16.96	.69	398	17.17	.63
399	17.72	-.01	400	16.13	.81	402	15.33	.87
403	12.92	1.49	404	16.71	.80	405	16.69	-.14
406	15.99	.85	407	15.80	-.01	408	16.78	-.15
409	13.44	.96	410	15.56	.85	411	16.02	-.08
412	16.07	.84	413	17.36	.84	414	17.22	.69
415	14.97	.92	416	15.86	-.03	417	16.45	.81
418	15.22	.11	419	16.25	-.07	420	15.38	.86
421	15.26	.12	422	15.74	.87	423	16.52	.80
424	15.77	0.00	425	14.82	.90	426	15.45	.83
427	16.19	.86	428	17.28	.67	430	15.95	-.06
431	15.22	.15	432	15.29	.12	433	15.94	.76
434	15.45	.85	435	15.47	.12	436	15.74	.05
437	15.86	.86	438	15.74	.01	439	16.36	-.08
440	16.23	.84	441	15.50	.02	442	15.29	.87
443	16.54	.69	444	17.21	.76	445	14.39	.65
446	14.81	.94	447	15.64	.02	448	17.10	.77
449	16.64	.72	450	17.27	.24	451	15.16	.92
452	17.58	.70	453	17.45	.76	454	17.52	.63
455	15.28	.90	456	15.85	.82	457	15.21	.19
458	15.86	-.07	459	15.48	.86	460	17.88	.46
461	17.72	.68	462	17.92	.73	463	16.73	.83
464	18.11	.69	465	17.63	.68	467	17.88	.86
468	17.93	.38	469	17.31	.73	470	17.18	.82
471	18.18	.69	474	17.11	.67	475	16.85	.77
476	15.99	-.04	477	16.96	-.10	478	17.81	.48
479	17.31	.75	480	15.64	.03	481	17.79	.69
482	17.98	.74	483	17.34	.64	484	16.22	.79
485	17.60	.80	486	16.90	-.13	487	15.91	.83
488	16.92	.79	489	16.27	.79	490	15.97	.77
491	16.01	.83	492	15.70	.01	493	14.51	.77
494	15.85	.85	495	17.75	.76	496	14.17	.55
497	16.45	-.05	498	18.09	.70	499	16.50	.85
500	17.44	.89	501	17.00	.73	502	17.98	.54
503	15.12	.89	504	15.87	-.02	506	16.74	.76
507	17.86	.43	508	15.70	.82	509	15.93	-.05
510	15.44	.86	511	16.97	.72	512	17.62	.26
513	17.15	-.15	514	15.21	.14	515	15.39	.61
516	15.87	-.05	517	16.31	.82	518	16.09	.81
519	16.05	.85	520	16.59	-.10	521	14.32	.73
522	16.11	.81	523	15.82	-.02	524	16.05	-.07
525	13.90	1.09	526	16.86	.83	528	15.67	.82
530	16.01	.85	531	12.96	1.66	532	16.12	.94
533	13.94	.89	534	16.10	.82	535	16.27	.74
536	16.47	.81	537	15.94	.87	538	17.26	.70
539	15.37	.83	540	17.09	.78	541	15.49	.86
542	16.82	.76	543	16.61	.89	544	14.88	.92
545	17.00	.76	546	15.35	.07	547	15.20	.89
548	16.89	.70	549	16.64	.90	550	18.07	.56
551	18.22	.74	552	17.16	.82	553	17.85	.69
554	16.81	1.36	555	16.49	.81	556	17.24	.79
557	17.37	.79	558	17.54	.67	559	17.34	.74
560	15.71	.01	561	16.29	1.01	562	15.80	-.06
563	14.78	-.05	564	16.67	.81	568	16.73	.77
569	15.53	.80	573	15.44	.92	574	17.04	.66
575	15.81	.84	577	15.60	-.02	580	15.46	.83
581	18.14	.66	584	18.15	.55	585	18.14	.65
586	18.00	.68	587	17.41	.69	589	18.20	.75
590	18.24	.77	592	18.20	.71	596	12.44	.85
599	17.42	.75	600	17.41	-.19	601	14.13	.89

of ~100 main-sequence stars, measure the turnoff position at $V_{to} \approx 19.0$, $(B-V)_{to} \approx 0.45$, in substantial agreement with our results. Finally, Buonanno *et al.* (1984), in a reworking of the Alcaino-Liller photographic plates, determine $V_{to} \approx 18.8$–19.0, $(B-V)_{to} \approx 0.44$; their study appears comparable in precision to ours. In summary, we believe that no major discrepancies now exist (at ± 0.2 in magnitude and ± 0.03 in color) among the various recent data sets defining the NGC 288 main sequence. However, a final resolution of any remaining small differences will have to await a more thorough and direct photometric calibration for $V > 18.0$.

The foreground reddening for NGC 288 (and the South Galactic Pole) has been discussed by several authors: Eggen (1970) used blue stars in the direction of the SGP, Lloyd Evans (1970) observed red giants in the same region, Cannon (1974) employed the two-color diagram for stars in NGC 288 itself, and Burstein and Heiles (1978) calculated E_{B-V} from the H I column density in the direction of NGC 288. All these studies

TABLE 4

PHOTOGRAPHIC DATA FOR BUTCHER STANDARDS

Star	V_{pg}	$(B-V)_{pg}$	ΔV(OCH-Butcher)
1	19.16	0.39	0.10
2[a]	19.42	0.51	0.06
3[a]	20.73	0.73	−0.50
4[a]	double		
5	19.77	0.50	−0.07
6[a]	20.34	1.05	−0.44
7	20.19	0.25	0.15
8	19.96	0.51	−0.02
9	19.08	0.49	−0.17
10[a]	double		
11	20.01	0.58	0.09
12	19.41	0.54	−0.08
13	18.83	0.44	0.09
14	20.60	0.80	0.21
15	18.59	0.44	0.02

[a] Not used for calibration.

TABLE 5

MEAN LINES FOR NGC 288 COLOR-MAGNITUDE DIAGRAM

V	$B-V$
12.60	1.50
12.80	1.40
13.13	1.30
13.50	1.20
14.00	1.10
14.50	1.00
15.15	0.90
16.05	0.80
16.80	0.75
18.00	0.70
18.25	0.65
18.35	0.60
18.60	0.50
18.80	0.45
19.00	0.44
19.20	0.44
19.50	0.45
19.90	0.50
20.15	0.60
21.00	0.66
...	...
15.30	0.21
16.00	0.03
17.00	−0.12

give closely consistent values of $E_{B-V} = 0.03 \pm 0.01$, which we shall adopt here. With $V_{HB} = 15.3$ and $M_V(\text{HB}) \approx 0.6$ from the main-sequence fit (see § V below), the distance modulus of NGC 288 becomes $(m - M)_0 = 14.6$, corresponding to $d = 8.3$ kpc.

IV. ABUNDANCE PARAMETERS

Aside from the various C-M studies, several recent independent investigations of NGC 288 have been made to determine its chemical composition by measuring its individual giant stars. These are listed below in rough chronological order.

a) *Washington system photometry:* The CMT_1T_2 photometric system (Canterna 1976; Harris and Canterna 1979) allows heavy-element abundances to be determined for late-type stars given their surface gravity and membership. Observations of several candidate NGC 288 giants in this system were taken with the 0.9 m and 1.5 m telescopes at CTIO during 1974 October and 1975 October, with the same cold box and filter combination that were used to define the system. Our measurements and estimted errors are listed in Table 6, along with the derived metallicities for those stars which do appear to be cluster members on the basis of our C-M diagram. The [Fe/H] values from the $M - T_1$ color index

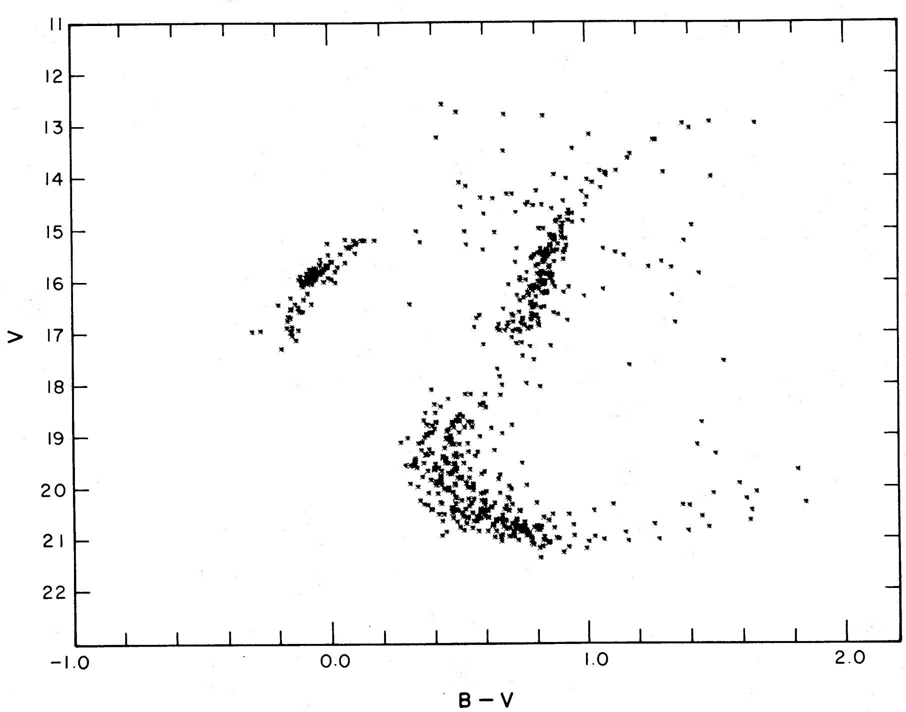

FIG. 5.—Composite color-magnitude diagram of NGC 288

TABLE 6

WASHINGTON SYSTEM PHOTOMETRY

Star	C-M	M-T_1	T_1-T_2	n	[Fe/H]$_{C\text{-}M}$	[Fe/H]$_{M\text{-}T_1}$
7	1.616	1.114	0.741	4		
8	1.278	0.867	0.609	1	−1.0	−1.4
36	1.269	0.837	0.613	4	−1.1	−2.1
38	0.925	0.742	0.451	3	−0.3	−0.3
41	1.070	0.784	0.556	3	−1.3	−1.4
26	1.254	0.846	0.616	1	−2.1	−2.4
28	1.020	0.786	0.535	2	−1.1	−1.7
23	0.948	0.711	0.553	1	−2.0	−3.0
20	1.673	1.041	0.704	1	−0.7	−1.7
Error (est.)	0.020	0.020	0.015		0.5	0.5

TABLE 7

CMD PARAMETERS FOR SELECTED GLOBULAR CLUSTERS

NGC	[Fe/H][a]	$(B-V)_{o,g}$	ΔV	S	$(B-V)_{o,\text{to}}$	$\Delta V_{\text{to-MB}}$
104 (47 Tuc)	−1.2	0.98	1.8	3.3	0.52	3.5
288	−1.2	0.85	2.6	4.7	0.40	3.8
5272 (M3)	−1.7	0.80	2.8	5.0	0.39	3.5
5904 (M5)	−1.3	0.81	2.6	4.6	0.41	3.4
6205 (M13)	−1.5	0.82	2.8	5.3	0.40	3.5
6341(M92)	−2.3	0.68	3.2	5.7	0.36	3.4

[a] High-dispersion spectroscopic abundances from Cohen (1978, 1979), Pilachowski, Sneden, and Canterna (1980), Pilachowski and Sneden (1980), and Pilachowski, Wallerstein, and Leep (1980).

(which measures metallic line blanketing) and from the $C-M$ index (metallic lines plus CN and CH) can be seen to differ systematically, in the sense that CN or CH appears to be enhanced relative to the metals ([Fe/H] ≈ -1.7, [CNO/H] ≈ -1.2), with a large (0.7 dex) spread in this latter abundance.

b) *High-dispersion spectra:* Pilachowski and Sneden (1980) have reported from curve-of-growth analyses of some of the brightest giants in NGC 288 that the oxygen abundance is relatively higher than the metals, i.e., [O/Fe] ≈ 0.5, and also (more surprisingly) that the basic metallicity is [Fe/H] ≈ -1.2, quite similar to the same quantities for the classic "metal-rich" globular cluster 47 Tuc. Although the metal-rich end of the globular cluster abundance scale is still a subject of much discussion (see PSW; Cohen and Frogel 1982), the essential issue for NGC 288 is that its weak-lines echelle features appear similar in strength to those of 47 Tuc.

c) *Spectrum scans:* McClure and Hesser (1981), from IIDS spectra of five NGC 288 giants, suggest that the cluster is intermediate in metallicity between M5 and 47 Tuc. This conclusion is based on DDO-system indices synthesized from the scans and on the strength of the most conspicuous features in the spectra (H and K lines, and CH absorption). More recently, Canterna, Harris, and Ferrall (1982) have analyzed CTIO vidicon spectra of 11 NGC 288 giants with roughly similar conclusions: they find that the CH, Ca, and Fe strengths are all consistent with an overall heavy-element abundance noticeably less enriched than 47 Tuc and slightly more enriched than M2. They obtain [Fe/H] (NGC 288) $= -1.4 \pm 0.2$, with additional evidence for variable star-to-star CN strength along the giant branch. The actual [Fe/H] value estimated from the spectral scans is close to that from the high-dispersion (weak-line) data quoted above, but the disagreement between them is actually severe in the sense that NGC 288 is plainly much less enriched *relative to 47 Tuc* according to strong-line features. Much more extensive comments on this fundamental and general problem are well known in the recent literature (e.g., see *IAU Colloquium No. 68*, Philip and Hayes 1981; Bell and Gustaffson 1982; and PSW). Though the results from all the preceding work are qualitatively similar in suggesting variable or enhanced CN by a factor of 3 over the metal lines, the actual [Fe/H] value is thus still somewhat hard to settle on. In what follows we will use [Fe/H] $= -1.3$ for NGC 288.

d) *CMD parameters:* The various CMD morphological parameters that have traditionally been regarded as abundance indicators, such as $(B-V)_{o,g}$ (Sandage and Smith 1966), ΔV (Sandage and Wallerstein 1960), the slope S (Hartwick 1968), or the turnoff color $(B-V)_{\text{to}}$ (Sandage 1970), cannot be used here to determine [Fe/H] independently since their properties are in part the very problem under discussion. Nevertheless, it is instructive to note how they compare with the parameters from certain other standard clusters (Table 7 and Figure 6). The turnoff region of NGC 288 matches that of M3 (Sandage 1970) in both color and shape quite well (but note that if we match up the HB luminosity of NGC 288 with that of M3, its turnoff luminosity then disagrees with that of M3. This problem may still reflect uncertainties in the calibration of the faint photometry.) The small differences in shape of the bluest part of the HB between NGC 288 and the other clusters (see Fig. 6) are likely not to be significant, given that no photoelectric standards of this blue are available in the NGC 288 field, and that the photographic scatter there is relatively large. The GB parameters for NGC 288 as listed in Table 7 all suggest a *slightly* higher metallicity for NGC 288 than for M13 or M3, but still much lower than 47 Tuc. Finally, the extremely blue HB is not expected in an object of 47 Tuc-type abundance. These clear differences between the CMD indicators and the high-dispersion spectroscopic abundances [part (*b*) above] emphasize the discrepancy discussed in the previous section.

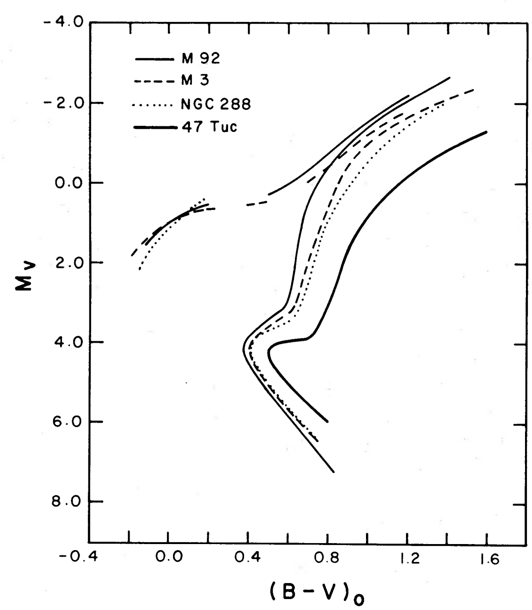

FIG. 6.—The mean color-magnitude relations for the clusters M92, M3, 47 Tuc, and NGC 288.

V. DISCUSSION

The basic "anomaly" represented by NGC 288 remains the extremely blue horizontal branch distribution in a cluster which is moderately (though not extremely) metal-rich. One obvious possibility would be that NGC 288 may have a helium abundance higher than in comparison clusters such as M3 or M13. As indicated by the synthetic "clusters" of Rood (1973) or Demarque (1980), the HB color distribution is sensitive to helium for ages near 10^{10} yr; the HB of a globular cluster with a basic metallicity of [A/H] ~ -1 can be shifted from red to completely blue by a change in helium composition of $\Delta V \sim 0.1$. In addition, NGC 288 has relatively few red giants compared with HB stars ($N_{HB}/N_{RG} \approx 2.0$), which again is a rough indicator of high Y (Iben *et al.* 1969; Demarque, Sweigart, and Gross 1972). The effects of increasing Y by ~ 0.1 would both make the HB brighter by 0.1–0.2 mag (Demarque and McClure 1980; Sweigart and Gross 1978) and the turnoff fainter by ~ 0.3 mag, so that the difference ΔV (turnoff-HB) will increase with Y. A secondary effect on the turnoff is that its color $(B-V)_{to}$ also becomes bluer with increasing helium (by roughly 0.04 mag for $Y \sim 0.1$). However, the uncertainties in our photometric calibration for the main-sequence region (see § II above) are still too high to give this hypothesis much substance. As will be seen below, isochrone fits within a more "normal" set of parameters are capable of matching the main sequence and subgiant colors adequately.

The competing possibility of a different age T for NGC 288 should also be mentioned, since significant age differences between clusters with well-established main-sequence data have been proposed (cf. Demarque and McClure 1977; Carney 1980, 1981, among others). An extreme age would also produce a blue HB (by reducing the average stellar mass of the HB stars) and a somewhat fainter turnoff for a given heavy-element abundance. But this alternative would then lead to a new set of problems if Y does not *also* change: for example, NGC 288 cannot have a composition (Fe, CNO, Y) similar to either M3 or 47 Tuc and a larger age than either of them, and yet have a main-sequence turnoff color *identical* with M3 and *bluer* than 47 Tuc [since $(B-V)_{to}$ increases with T by ≈ 0.02 mag every 10^9 yr].

This argument essentially reflects the basic difficulties encountered once one deviates significantly from a "normal" set of age and composition parameters (see, e.g., VandenBerg 1983); to reachieve a successful isochrone match, one must then adopt "unusual" values for *more* than one parameter.

We have carried out trial isochrone fits to our NGC 288 data. Our best fit, using the models of VandenBerg (1983), was obtained for the composition of $Y = 0.2$, $M_V(\mathrm{HB}) = 0.6$, and age $T = (15 \pm 3) \times 10^9$ yr with $Z = 0.001$ (corresponding to [Fe/H] ≈ -1.3 for $Z_0 = 0.02$). Adopting a *higher* Z forces the main-sequence fit into a lower age and a brighter HB luminosity. For $Z > 0.002$ or $Y < 0.2$, we would obtain results that we regard as untenable (i.e., $M_V(\mathrm{HB}) < 0$; $T < 10 \times 10^9$ yr). Conversely, if $Z \leq 0.0005$, then the derived cluster age becomes larger than 18×10^9 yr. Thus the isochrone fit itself yields approximate constraints on the abundance Z which are within the observed range quoted in § III. The slight difference in our best age estimate compared with that of Alcaino and Liller (1980*b*) is due mainly to our revised turnoff location, as mentioned above. By comparison, use of the Iben and Rood (1970) interpolation formula for cluster age would give us $T = 16 \times 10^9$ yr with $Y = 0.3$, $Z = 0.002$, and log $L_{to} = 0.17$.

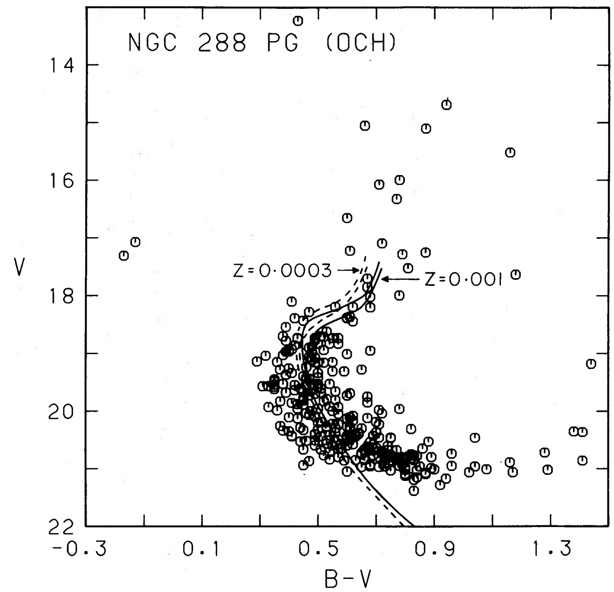

FIG. 7.—The main-sequence portion of the CMD, overlaid by isochrone fits for $Z = 0.001$ and $Z = 0.003$. For each composition, ages of 15×10^9 and 18×10^9 yr are shown. In each case, the younger age is the brighter and bluer isochrone.

Our isochrone fits are shown in Figure 7. The turnoff region of the color-magnitude diagram is overlaid by VandenBerg's (1983) isochrones for the compositions $Y = 0.2$, $Z = (0.001$ and $0.0003)$, and ages $T = 15$ and 18×10^9 yr. We have *not* arrived at the fit shown here by an exhaustive exploration of all possible model choices within the VandenBerg set (cf. the approach of Flannery and Johnson 1982). Our aim here is only to stress that a relatively "normal" interpretation of the NGC 288 main-sequence and giant branch (i.e., age T similar to that of well-studied clusters, and [Fe/H] similar to the bulk of the data discussed earlier) is possible within the current errors of observation. A considerably more precise definition of the main sequence will be needed to pin these parameters down with more reliability.

The authors would like to thank Dr. Martha Liller for the loan of her plates and Dr. Paul Hodge for crucial help with the observations, Dr. R. McClure for valuable discussions, Dr. H. Butcher for advance use of his photometric sequence, and Dr. R. Cannon for transmitting his electronographic color-magnitude data at an early stage. Financial assistance from the University of Washington Computer Center to reduce the data is gratefully acknowledged. This work was supported in part by the National Sciences and Engineering Research Council, through operating grants to W. E. Harris, and through research grant NSF AST 81-2952 to Paul Hodge.

REFERENCES

Alcaino, G., and Liller, W. 1980*a*, *A.J.*, **85**, 680.
———. 1980*b*, *A.J.*, **85**, 1592.
Bell, R. A., and Gustaffson, B. 1982, *Ap. J.*, **255**, 122.
Blanco, V. 1982, *Publ. A.S.P.*, **94**, 201.
Buonanno, R., Corsi, C. E., Fusi-Pecci, F., Alcaino, G., and Liller, W. 1984, *Ap. J.*, **277**, 220.
Burstein, D., and Heiles, C. 1978, *Ap. J.*, **225**, 40.
Butcher, H. 1980, private communication.

Cannon, R. 1974, *M.N.R.A.S.*, **167**, 551.
———. 1981, in *Astrophysical Parameters for Globular Clusters, IAU Colloq. 68*, ed. A. G. D. Philip and D. S. Hayes (Schenectady: L. Davis Press), p. 501.
Cannon, R., and Hawkins, M. R. S. 1983, private communication.
Canterna, R. 1976, *A.J.*, **81**, 228.
Canterna, R., Harris, W. E., and Ferrall, T. 1982, *Ap. J.*, **258**, 612.
Carney, B. W. 1980, *Ap. J. Suppl.*, **42**, 481.
———. 1981, *Astrophysical Parameters for Globular Clusters, IAU Colloq. No. 68*, ed. A. G. D. Philip and D. S. Hayes (Schenectady: L. Davis Press), p. 477.
Christian, C. A., and Racine, R. 1983, *Pub. A.S.P.*, **95**, 457.
Cohen, J. 1978, *Ap. J.*, **223**, 487.
———. 1979, *Ap. J.*, **231**, 751.
———. 1980, *in Star Clusters, IAU Symposium No. 85*, ed. J. E. Hesser (Dordrecht: Reidel), p. 385.
Cohen, J. G., and Frogel, J. A. 1982, *Ap. J.* (*Letters*), **255**, L39.
Demarque, P. 1980, in *Star Clusters, IAU Symposium No. 85*, ed. J. E. Hesser (Dordrecht: Reidel), p. 281.
Demarque, P., and McClure, R. D. 1977, in *Evolution of Galaxies and Stellar Populations*, ed. B. M. Tinsley and R. B. Larson (New Haven: Yale University Observatory), p. 199.
Demarque, P., and McClure, R. D. 1980, *Ap. J.* (*Letters*), **242**, L5.
Demarque, P., Sweigart, A. V., and Gross, P. G. 1972, *Nature*, **239**, 85.
Deupree, R. G., Eoll, F. G., Hodson, S. W., and Whitaker, R. W. 1978, *Pub. A.S.P.*, **90**, 53.
Eggen, O. J. 1970, *Ap. J. Suppl.*, **22**, 289.
Faulkner, J. 1966, *Ap. J.*, **144**, 978.
Flannery, B. P., and Johnson, B. C. 1982, *Ap. J.*, **263**, 166.
Friel, E., Kraft, R. P., Suntzeff, N. B., and Carbon, D. F. 1982, *Pub. A.S.P.*, **94**, 873.
Green, E. M. 1980, in *Star Clusters, IAU Symposium No. 85*, ed. J. E. Hesser (Dordrecht: Reidel), p. 441.
Harris, H. C., and Canterna, R. W. 1979, *A.J.*, **84**, 1750.
Harris, W. E., and Canterna, R. 1980, *Ap. J.*, **239**, 815.
Harris, W. E., Hesser, J. E., and Atwood, B. 1983, *Pub. A.S.P.*, **95**, 951.
Harris, W. E., and Pateman, D. 1979, private issued manuscript, McMaster University.
Hartwick, F. D. A. 1968, *Ap. J.*, **154**, 475.
Hawkins, M. R. S. 1979, *M.N.R.A.S.*, **188**, 691.
———. 1981, *M.N.R.A.S.*, **194**, 1013.
Hesser, J. E., and Hartwick, F. D. A. 1977, *Ap. J. Suppl.*, **35**, 361.
Hollingsworth, L. M., and Liller, M. H., 1977, *Inf. Bull. Var. Stars*, No. 1360, 3.
Iben, Jr., I., and Rood, R. T. 1970, *Ap. J.*, **159**, 605.
Iben, Jr., I. Rood, R. T., Strom, K. M., and Strom, S. E. 1969, *Nature*, **224**, 1006.
Lee, S. W. 1977, *Astr. Ap. Suppl.*, **27**, 381.
Lloyd Evans, T. 1970, *M.N.R.A.S.*, **149**, 311.
McClure, R. D., and Hesser, J. E. 1981, *Ap. J.*, **246**, 136.
Philip, A. G. D., and Hayes, D. S. 1981, *Astrophysical Parameters for Globular Clusters, IAU Colloquium No. 68*, ed. A. G. D. Philip and D. S. Hayes (Schenectady: L. Davis Press).
Pickering, E. 1891, *Ann. Harvard College Obs.*, **26**, xiv.
Pilachowski, C. A., and Sneden, C. 1980, *Bull. AAS*, **12**, 502.
Pilachowski, C. A., Sneden, C., and Canterna, R. 1980, in *Star Clusters, IAU Symposium No. 85*, ed. J. E. Hesser (Dordrecht: Reidel), p. 467.
Pilachowski, C. A., Sneden, C., and Wallerstein, W., 1983, *Ap. J. Suppl.*, **52**, 241 (PSW).
Pilachowski, C. A., Wallerstein, G., and Leep, E. M., 1980, *Ap. J.*, **236**, 508.
Racine, R., 1969, *A.J.*, **74**, 1073.
Rood, R. T., 1973, *Ap. J.*, **184**, 815.
Sandage, A. 1970, *Ap. J.*, **162**, 841.
———. 1982, *Ap. J.*, **252**, 553.
Sandage, A., and Smith, L. L. 1966, *Ap. J.*, **144**, 886.
Sandage, A., and Wallerstein, G. 1960, *Ap. J.*, **131**, 598.
Sandage, A., and Wildey, R. L. 1967, *Ap. J.*, **150**, 469.
Sawyer Hogg, H. 1973, *Pub. David Dunlap Obs.*, **3**, No. 6.
Stetson, P., and Harris, W. E. 1977, *A.J.*, **82**, 954.
Suntzeff, N. B. 1981, *Ap. J. Suppl.*, **47**, 1.
Sweigart, A. V., and Gross, P. G., 1978, *Ap. J. Suppl.*, **36**, 405.
VandenBerg, D. A., 1983, *Ap. J. Suppl.*, **51**, 29.

RONALD W. CANTERNA: Department of Physical Education, Biomechanics Laboratory, University of Iowa, Iowa City, IA 52242

WILLIAM E. HARRIS: Department of Physics, McMaster University, Hamilton, Ontario L8S 4M1, Canada

EDWARD W. OLSZEWSKI: Dominion Astrophysical Observatory, Herzberg Institute of Astrophysics, 5071 W. Saanich Road, Victoria, B.C. V8X 4M6, Canada